Title

AN INTEGRATED FINITE DIFFERENCE METHOD FOR ANALYZING FLUID FLOW IN POROUS MEDIA

Authors

Narasimhan, T.N.
Witherspoon, P.A.

Publication Date

1975-04-01

Submitted to Water Resources Research

LBL-3258
Preprint c. 1

AN INTEGRATED FINITE DIFFERENCE METHOD FOR ANALYZING FLUID FLOW IN POROUS MEDIA

T. N. Narasimhan and P. A. Witherspoon

April 1975

Prepared for the U. S. Energy Research and Development Administration under Contract W-7405-ENG-48

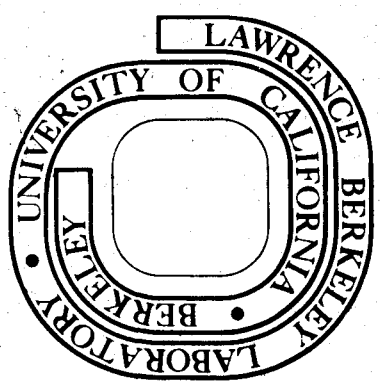

DISCLAIMER

AN INTEGRATED FINITE DIFFERENCE METHOD FOR ANALYZING FLUID FLOW IN POROUS MEDIA

by

T. N. Narasimhan, Department of Civil Engineering

and

P. A. Witherspoon, Lawrence Berkeley Laboratory
University of California, Berkeley, California 94720

Abstract

The theoretical basis for the integrated finite difference method (IFDM) is presented to describe a powerful numerical technique for solving problems of groundwater flow in porous media. The method combines the advantages of an integral formulation with the simplicity of finite difference gradients and is very convenient for handling multi-dimensional, heterogeneous systems composed of isotropic materials. Three illustrative problems are solved to demonstrate that two- and three-dimensional problems are handled with equal ease. Comparison of IFDM with the well known finite element method (FEM) indicates that both are conceptually similar and differ only in the procedure adopted for measuring spatial gradients. The IFDM includes a simple criterion for stability and an efficient explicit-implicit, iterative scheme for marching in the time domain. If such a scheme can be incorporated in a new version of FEM, it should be possible to develop an improved numerical technique that combines the inherent advantages of both methods.

Introduction

Numerical analysis of fluid flow through porous media in problems with complex geometry is greatly facilitated by the use of integral formulations. Perhaps the most widely used integral method is the Finite Element Method (FEM), which can be based on variational principles or the Galerkin approach.

In this paper we will describe another integral formulation which has been successfully used to solve heat transfer problems in heterogeneous, isotropic, multi-dimensional flow regions. For reasons that will become clear later, we shall call this method the "Integrated Finite Difference Method" (IFDM). Although the method has been used in studying groundwater systems [Todd, 1959; Cooley, 1971] it does not appear to have been widely employed in the field of hydrogeology. It is our opinion, however, that the IFDM can be a very powerful tool in analyzing heterogeneous groundwater systems with complex geometries. Furthermore, in comparing the conceptual bases of IFDM and FEM, we find that they have much in common.

The purpose of this paper is first to develop the IFDM equations and demonstrate the power of the method with three different problems. We will then examine the conceptual bases of both IFDM and FEM and attempt to identify those features which give each of these techniques unique advantages in handling specific classes of problems. Finally, we will consider the possibility of developing a new technique which could combine some of the unique advantages of each method.

The Integrated Finite Difference Method

MacNeal [1953] is apparently the first worker to use the IFDM approach, and he classified it as an "asymmetric finite difference network". He used

this approach in solving second order boundary value problems. Subsequently, the method has been used successfully for solving heat transfer problems and a good description of the approach and related aspects can be found in Dusinberre [1961]. Edwards [1969] used the IFDM in developing a powerful computer code called TRUMP for calculating transient and steady state temperature distributions in multididimensional systems, and the following discussion will be based in large measure on the TRUMP program. Although TRUMP can handle conductive, convective, and radiative heat transfer, we will restrict our attention to the heat conduction part of the program since conductive heat transfer is conceptually similar to fluid flow in porous media.

Consider the partial differential equation for groundwater flow

$$\text{div } K \vec{\text{grad}}\, \phi + g = c \frac{\partial \phi}{\partial t} \tag{1}$$

For the sake of simplicity, we shall assume K and c in (1) to be constant and independent of ϕ so that (1) is a linear equation.

We can spatially integrate (1) over a conveniently small finite subregion V of the flow region and write [Encyclopedia of Science and Technology, 1960]

$$\int_V [\text{div } K \vec{\text{grad}}\, \phi + g]\, dV = \frac{\partial}{\partial t} \int_V c\phi dV \tag{2}$$

If it can be assumed that c, ϕ and g represent average values within the subregion, we can now use the divergence theorem to convert the first term on the left hand side of (2) to a surface integral and obtain

$$\int_S K \vec{\text{grad}}\, \phi \bullet \vec{n}\, dS + gV = cV \frac{\partial \phi}{\partial t} \tag{3}$$

The central concept of IFDM is to discretize the total flow domain into conveniently small subdomains or "elements" and evaluate the mass balance in each element as indicated in (3). Physically, the surface integral on the left hand side of (3) is the summation of fluxes over the surface S and thus measures the rate at which mass is accumulating in the element, as governed by initial and boundary conditions. The right hand side converts the rate of accumulation of fluid into the corresponding average time rate of change in potential over the element.

To illustrate the IFDM, let the shaded region in Figure 1 be an element whose average properties are associated with a representative nodal point m = 6, which may be located anywhere within or on the boundaries of the element. Maximum accuracy in transient problems is obtained if the element shapes and nodal point locations are so chosen that lines joining nodal points of adjacent elements are perpendicularly bisected by the common interface. In steady state problems, the solution is independent of the specific storage associated with each element, so the nodal points may be located anywhere without loss of accuracy. In Figure 1, element m is connected to adjoining elements n = 1 to 5. Under these conditions, the finite difference approximation for (3) can be written

$$g_m V_m + \sum_n \bar{K}_{m,n} \frac{\phi_n - \phi_m}{D_{m,n}} A_{m,n} = c_m V_m \frac{\Delta\phi_m}{\Delta t} \tag{4}$$

For appropriately small values of Δt, (4) can be written in explicit form as

$$\frac{\Delta t}{c_m V_m} \left[g_m V_m + \sum_n U_{m,n} (\phi_n - \phi_m) \right] = \Delta\phi_m \tag{5}$$

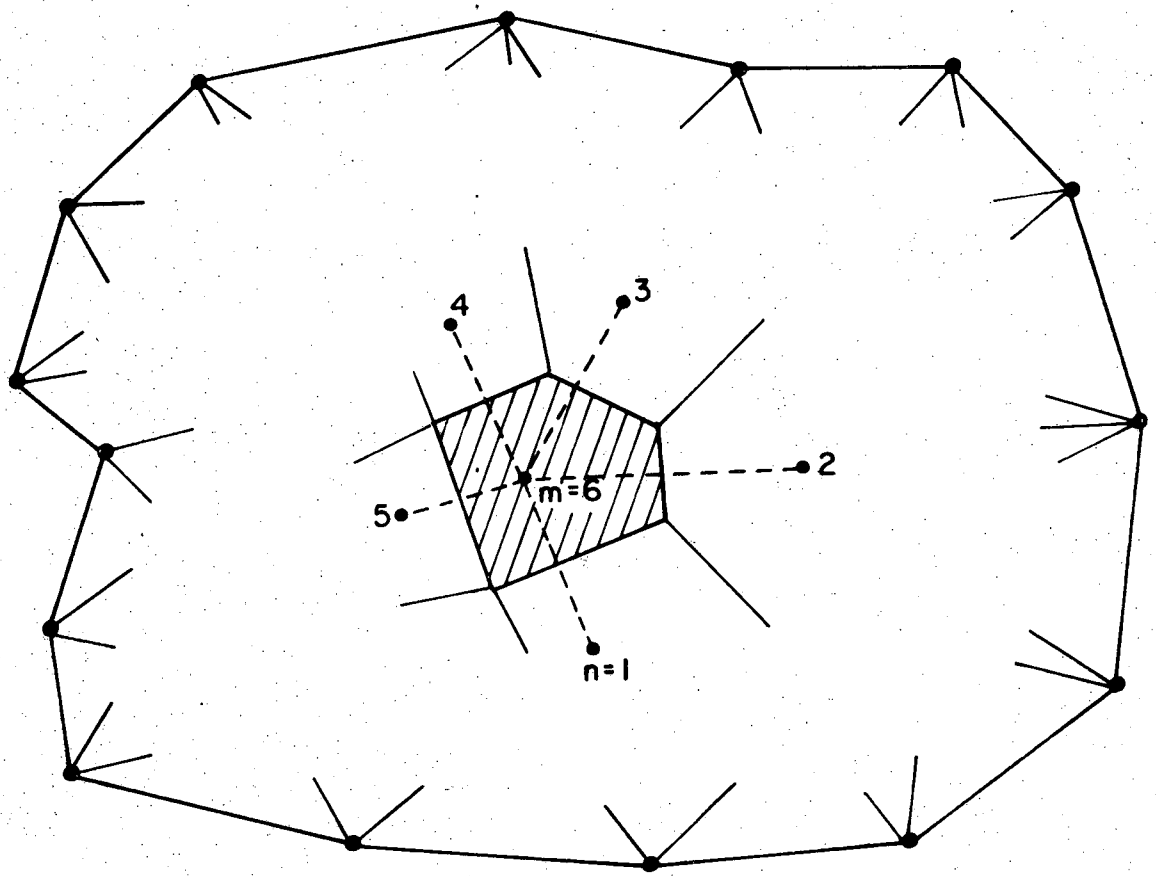

XBL 754-1093

Fig. 1. An element with its representative nodal point in the IFDM network.

Here, $U_{m,n} = (\bar{K}_{m,n} A_{m,n})/D_{m,n}$ is the "conductance" of the interface separating elements m and n, and represents the rate of fluid transfer per unit difference in potential between nodal points m and n. The terms ϕ_m and ϕ_n represent the initial values of potentials at the beginning of the interval Δt. Equation 5 can be directly used to solve for $\Delta\phi_m$ if the geometric parameters $A_{m,n}$, $D_{m,n}$ and V_m are provided as input data, in addition to the material properties, K and c.

If it is desired to use large values of Δt, then equation 6 can be expressed implicitly as

$$\frac{\Delta t}{c_m V_m} \left\{ g_m V_m + \sum_n U_{m,n} [(\phi_n + \lambda\Delta\phi_n) - (\phi_m + \lambda\Delta\phi_m)] \right\} = \Delta\phi_m \qquad (6)$$

where $0 < \lambda < 1$.

When $\lambda = 0$, (6) reduces to the forward differencing scheme (5). When $\lambda = 1$, (6) becomes a fully implicit, backward differencing scheme while $\lambda = \frac{1}{2}$ yields the well known central differencing, or Crank-Nicholson procedure. For unconditional stability, $\lambda > \frac{1}{2}$.

To handle boundary conditions, we can rewrite (6) as

$$\frac{\Delta t}{c_m V_m} [g_m V_m + \sum_n U_{m,n} (\bar{\phi}_n - \bar{\phi}_m) + \sum_b U_{m,b} (\bar{\phi}_b - \bar{\phi}_m)] = \Delta\phi_m \qquad (7)$$

where $\bar{\phi}_m = \phi_m + \lambda\Delta\phi_m$

$\bar{\phi}_n = \phi_n + \lambda\Delta\phi_n$

and b is used to distinguish boundary elements from the n elements in the interior. Using the last summation term on the left hand side of (7), both prescribed potential as well as prescribed flux boundaries or even mixed boundary conditions can be suitably handled, as described by Edwards [1969] and Narasimhan [1975].

It can be shown either from simple reasoning [Dusinberre, 1961] or based on an elaborate analysis of error propagation [O'Brien, et al., 1951; Evans, et al., 1954; Narasimhan, 1975] that for each element m there is a critical time constant Δt_m such that equation 5 is unstable if $\Delta t > \Delta t_m$. The magnitude of this critical time constant is given by

$$\Delta t_m = \frac{c_m V_m}{\sum_n U_{m,n}} \tag{8}$$

where n now stands for all elements connected to element m. Physically Δt_m represents the approximate time required for element m to react significantly to changes in potential in the adjacent elements to which m is connected [Edwards, 1969]. Obviously, if $\Delta t > \Delta t_m$ for any element m, one would have to use (6) or (7) instead of (5) for that particular element.

The implicit calculations inherent in the application of equation 7 can be carried out either with the help of matrix-inversion techniques or with the help of iterative techniques. The TRUMP computer program [Edwards, 1969] employs an iterative technique based on the generalization of a method suggested by Evans et al. [1954]. Using this approach and recognizing the fact that the critical time step Δt_m is defined for each element, Edwards [1969] has successfully incorporated in TRUMP a technique by which explicit calculations are carried out for those elements where $\Delta t < \Delta t_m$ and implicit calculations for the balance where $\Delta t > \Delta t_m$. The IFDM, when combined with the explicit-implicit, iterative scheme developed in TRUMP, provides a very useful tool in analyzing fluid flow problems in heterogeneous systems.

Solutions to Illustrative Problems

To illustrate the utility of the IFDM, we shall consider three problems for which analytical solutions are available. The first of these has been chosen to demonstrate the accuracy that can be expected from IFDM as compared to that of FEM. The second is designed to demonstrate the ability of IFDM to solve three dimensional problems. The last example serves to illustrate the use of the method in approaching systems with radially symmetric geometry, in which the material distribution can be asymmetric.

Theis Problem

A classical problem in the field of groundwater hydrology is that of nonsteady, radial flow to a well discharging at a constant rate, Q, and piercing a horizontally infinite, homogeneous and isotropic aquifer. The solution to this problem is the well known Theis [1935] equation

$$s = \frac{Q}{4\pi r} \int_{\frac{r^2 S}{4Tt}}^{\infty} \frac{e^{-u}}{u}\, du \qquad (9)$$

Pinder and Frind [1972] have shown how the FEM developed from the Galerkin formulation can be used to simulate the Theis solution. They verified the accuracy of their FEM results in comparison with the analytical solution using linear as well as isoparametric elements. Their FEM mesh consisted of only nine nodal points along any radial line from the well.

To check the accuracy of IFDM, we set up a mesh with the same number and a similar spacing of nodal points and solved the same problem. Figure 2 shows drawdown as a function of time, as computed by FEM and IFDM. A comparison of these numerical results with the analytical solution shows that IFDM results compare somewhat more favorably with the analytical solution than has been

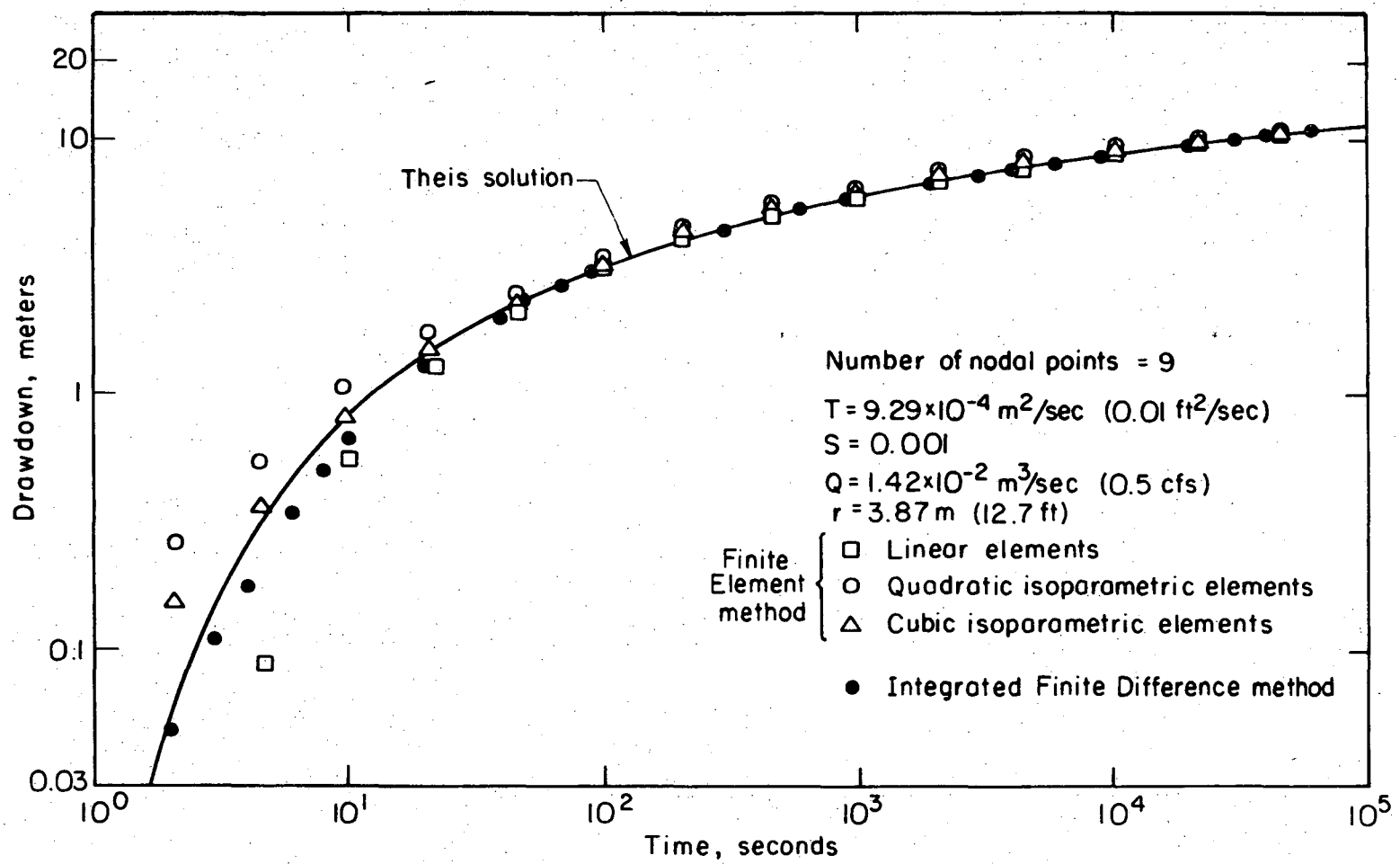

XBL 754-1094

Fig. 2. Comparison of numerical results with analytical solution for Theis problem.

reported by Pinder and Frind [1972] for their FEM approach.

Continuous Point Source Problem

An advantage of formulating the governing equation in the form of (5) or (6) is that these equations are equally valid in one, two or three dimensions. Therefore, the IFDM can handle one-, two- or three-dimensional problems with equal ease. To verify the ability of IFDM to handle three-dimensional flow, we applied the method to the problem of a continuous point source in an isotropic medium. The analytical solution is given by Carslaw and Jaeger [1959] as

$$\phi(r,t) - \phi_o(r,t_o) = \frac{Q}{4\pi K r} \operatorname{erfc}\left[\frac{r}{\sqrt{4Kt}}\right] \qquad (10)$$

To solve the above problem in three-dimensions using the IFDM, the flow region was visualized as a sphere enclosed in a cube. Thus, the spherical elements near the point source gradually lost their curvature in grading outward to cubic shaped elements at the outer boundary (Figure 3). This was done so that one could accurately simulate spherical symmetry close to the source, while allowing for more general conditions of flow near the outer limits. The flow region was everywhere subdivided into three-dimensional elements. From considerations of symmetry (eight octants in a cube and three cartesian axes), a wedge-shaped portion of the flow region, whose volume is 1/24 of a cube was chosen for actual modelling as illustrated in Figure 3.

The shortest distance from the point source to the outer boundary of the wedge was 400 m. The mesh consisted of 47 three-dimensional elements and 87 interfaces between elements. Due to the curvilinear nature of the elements, different nodal points were located along different radial lines from the

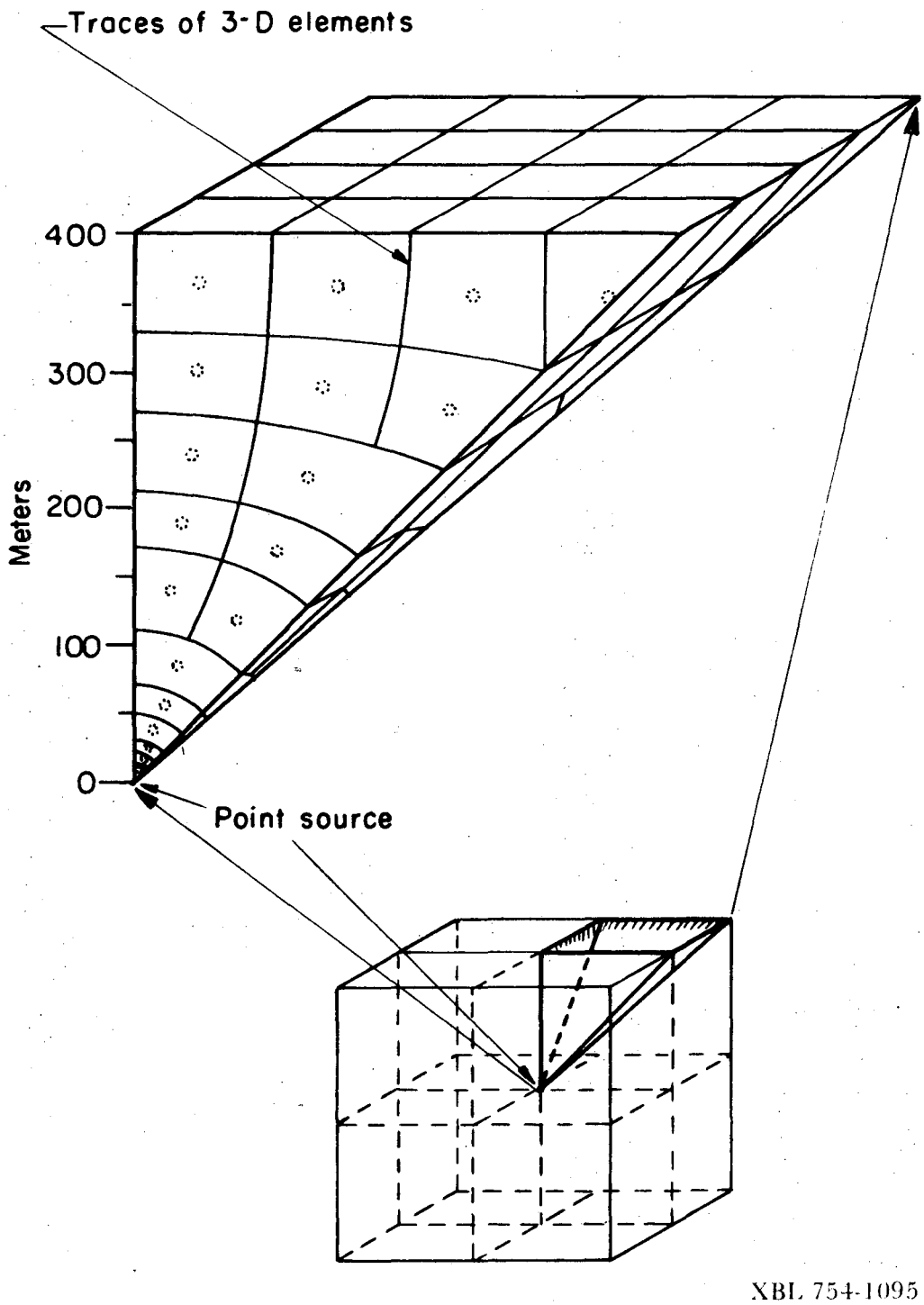

Fig. 3. Three-dimensional IFDM network of elements for point source problem.

point source. Distances from the source to nodal points varied from 1 m for the closest to 593 m for the farthest, while element volumes ranged from 9.1×10^{-1} to 1.09×10^{6} m^3. The problem was solved with the following, arbitrary parameters: $Q = 10^{3}$ m^3/sec, $K = 10^{-3}$ m/sec, and $c = 10^{-2}/m^{-1}$. Impermeable conditions were assumed on all faces of the wedge-shaped flow region.

The results of the computations are presented in Figure 4. In Figure 4A, drawdown as a function of time is compared to the analytical solution for various distances from the point source. In Figure 4B, drawdown as a function of distance is compared to the analytical solution for various values of time. The results pertain to points located on different radial lines and hence they give an idea of the overall accuracy of the solution over the entire mesh. The transient problem was solved from 0 to 10^{6} seconds in 683 time cycles. The magnitude of the time steps varied from 1×10^{-1} to 8.5×10^{3} seconds. The simulation took 8.5 seconds of CDC 7600 machine time.

Figures 4A and 4B show that the computed results deviate from the analytical solution for small values of time and at small radial distances. However, we believe that the overall agreement with the analytical solution is quite good, and we conclude that the IFDM has successfully been used in solving this three-dimensional problem.

Fracture Flow Problem

The parallel plate formulation for flow in a fracture is widely used by many workers [Snow, 1965; Romm, 1966; Louis, 1969; Sharp and Maini, 1972; and Wilson and Witherspoon, 1974; Gale et al., 1974] and leads to a fracture permeability defined as

$$k = \frac{\rho g b^2}{12\mu} \tag{12}$$

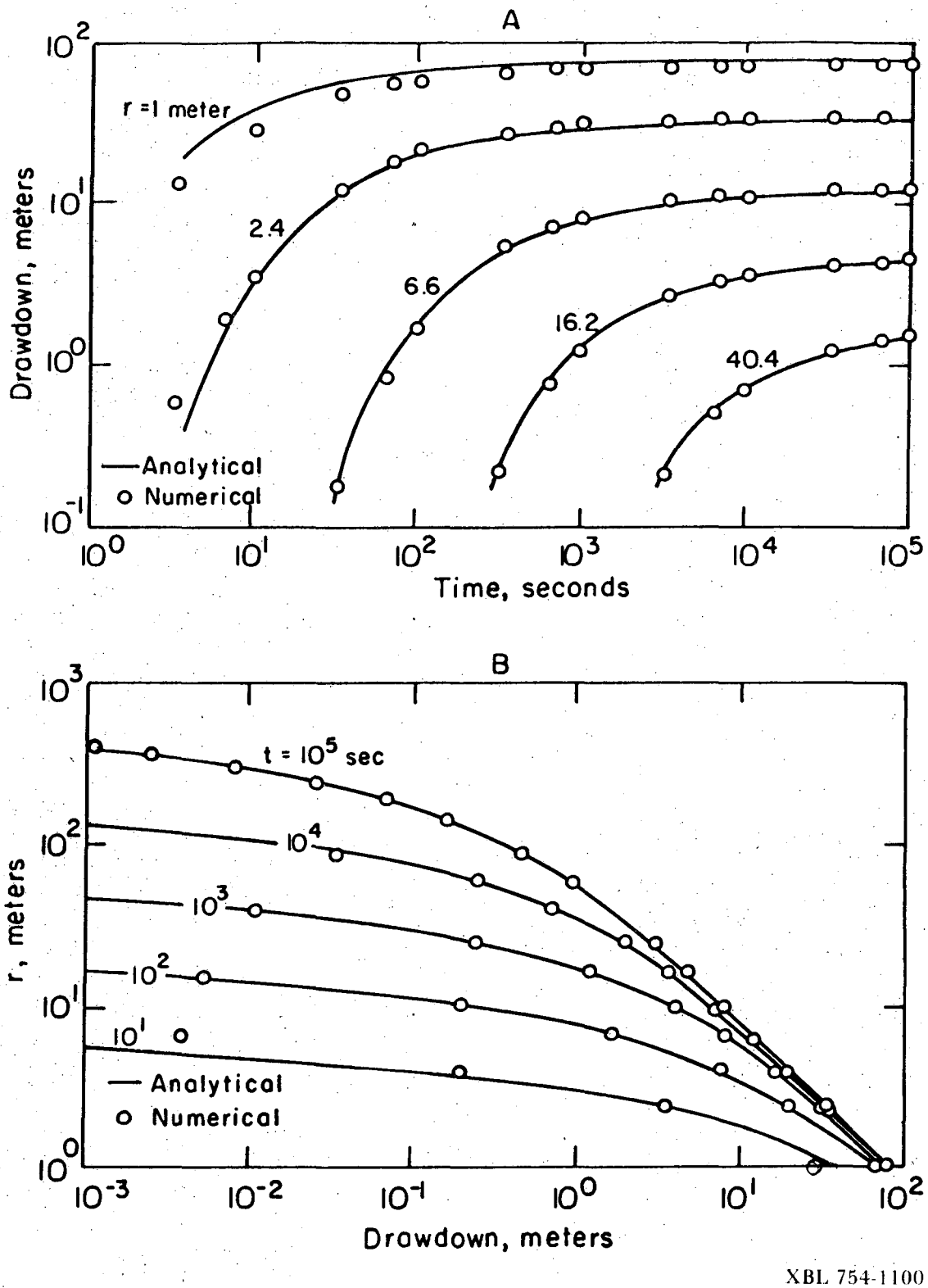

Fig. 4. Comparison of numerical results with analytical solution for point source problem: A, time drawdown; B, distance drawdown

However, when the fracture closes, the surfaces do not necessarily touch at every point, and this becomes quite obvious when any natural fracture is examined in detail. This has led some investigators [Louis, 1969; Sharp and Maini, 1972] to suggest that the exponent in (12) is some value less than 2 for a fracture that is being closed under normal stress.

In other work in this laboratory, we are currently investigating this problem using a single, horizontal fracture under conditions of radial flow. The fracture is formed by two cylindrical blocks of impermeable rock, .152 m in diameter, each having smooth faces. Flow originates at a .0254 m diameter hole in the center that is concentric with the external boundary. If the circular fracture is open and the planar surfaces are parallel, then the steady-state flow is given by

$$Q = \frac{2\pi \rho g b^3 \Delta\phi}{12\mu \ln(r_e/r_i)} \qquad (13)$$

To investigate this problem, we have used the IFDM and setup a flow net of elements as shown in Figure 5. The flow region has been discretized into 264 elements with 456 interfaces, and permeability within each element is given by (12).

As a practical problem of interest in the laboratory work, we solved an arbitrary case where $\Delta\phi$ = 21.09 m of water (30 psi), ρ = 1000 Kg/m^3, μ = .001 Kg/m sec and b = 1.27 x 10^{-4} m. From (13), one can quickly compute

$$Q = \frac{2\pi\ (1000)(9.8)(1.27 \times 10^{4})^{3}(21.09)}{12\ (.001)\ \ln\ (.076/.0127)} = 1.237 \times 10^{-4}\ \text{m}^3/\text{sec}$$

We then solved the same problem using IFDM and the network shown in Figure 5 and obtained Q = 1.227 x 10^{-4} cm^3/sec. Pressures should be a linear function of ln r and comparison of IFDM results with those from the analytical solution are shown in Figure 6. The agreement is very good.

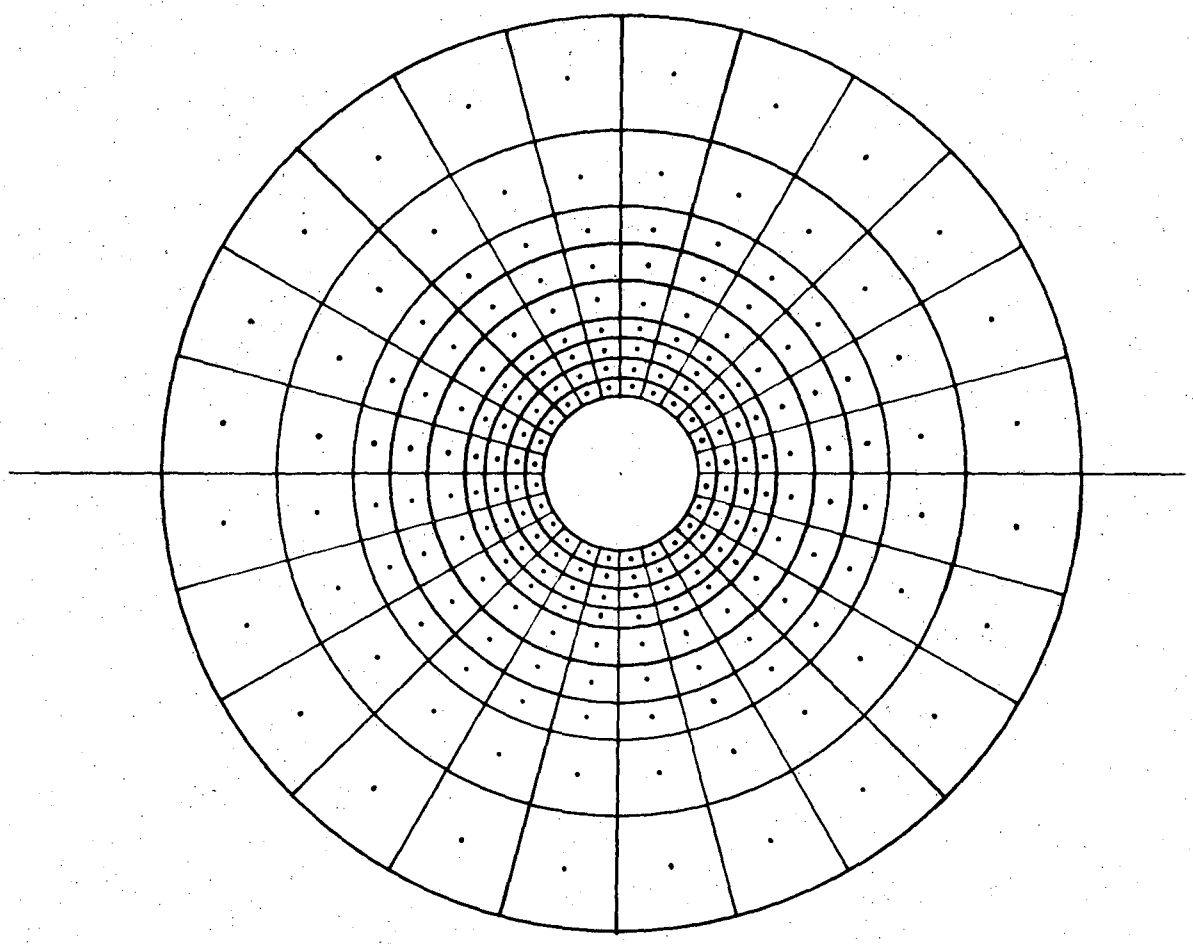

XBL 754-1097

Fig. 5. Two-dimensional IFDM network of elements for fracture flow problem

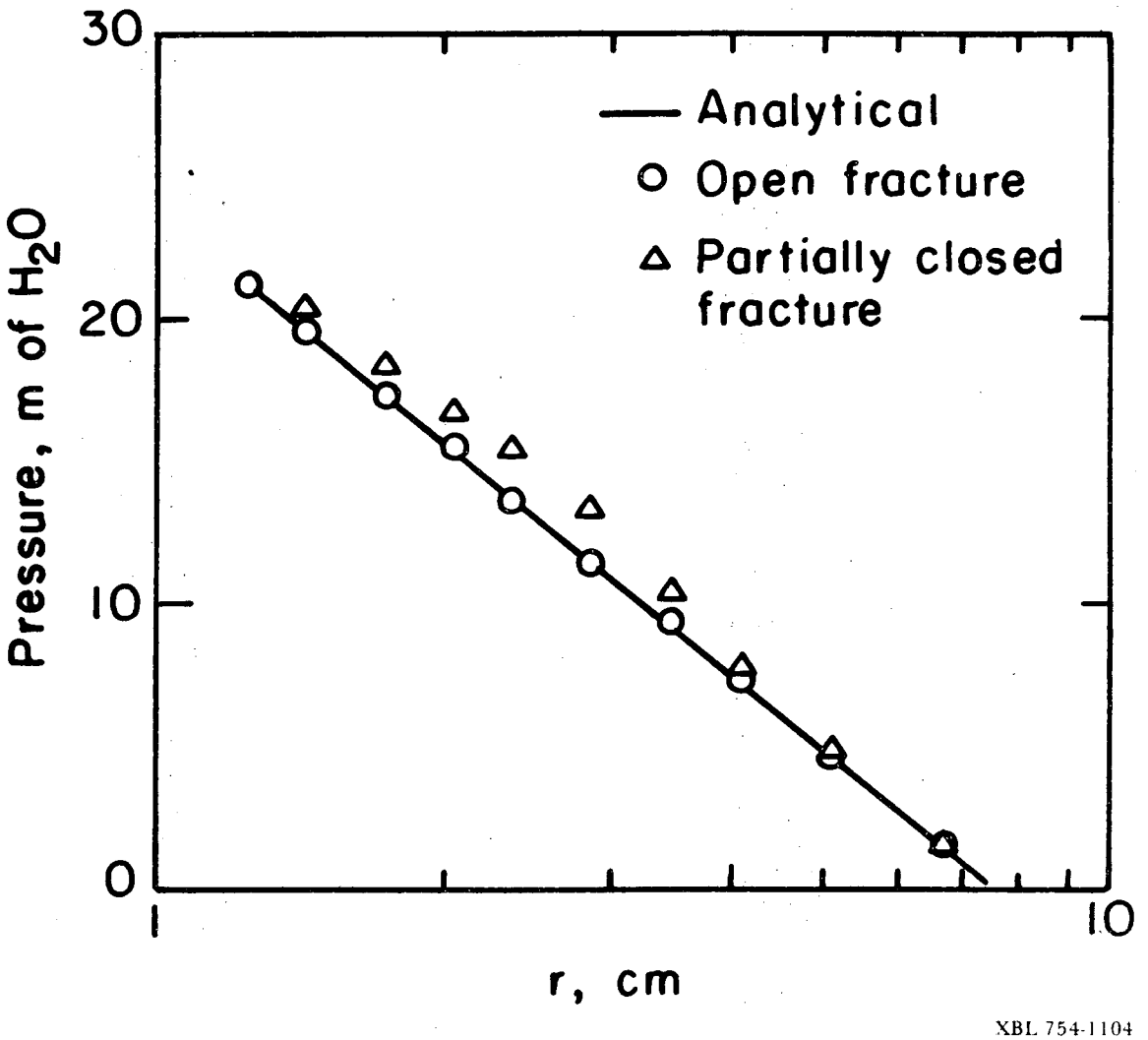

Fig. 6. Comparison of numerical results with analytical solution for fracture flow problem

Of considerably more interest is the case where the fracture partially closes and the areas of contact are impermeable. This is easily handled with the IFDM by assuming that certain elements within the network of Figure 5 have zero permeability. The results of a hypothetical problem with a random distribution of impermeable elements is given in Figure 7. Here, the pressure head has been normalized in terms of percent of the injection pressure. The pressure profile along line AB of Figure 7 is shown in Figure 6. For the same aperture and flow conditions as given above, the flow was found to be 8.032×10^{-5} m^3/sec. In other words, the impermeable contact area that amounts to about 15 percent of the total fracture surface caused a reduction in flow of approximately 35 percent. Computer simulations of carefully chosen hypothetical situations for this kind of fracture flow can provide valuable assistance in analyzing laboratory data.

Comparison of IFDM and FEM

From the above discussion, we have seen how the IFDM can be used to analyze transient fluid flow problems in multi-dimensional systems with complex geometry. The FEM is also well suited to such problems, and the question will arise as to how the two methods compare. A detailed analysis is not an easy task, and only a comparison of the overall features will be attempted here. Our purpose is to provide some clues when choosing an approach to certain classes of problems and also to provide an insight into the development of new techniques of analysis that will combine the inherent advantages of both IFDM and FEM.

Although FEM equations can be developed from variational principles [Javandel and Witherspoon, 1968] or physical considerations [Wilson, 1968], mathematically the most direct method is the Galerkin approach [Zienkiewicz and Parekh, 1970; Pinder and Frind, 1972; Neuman, 1973]. In the following

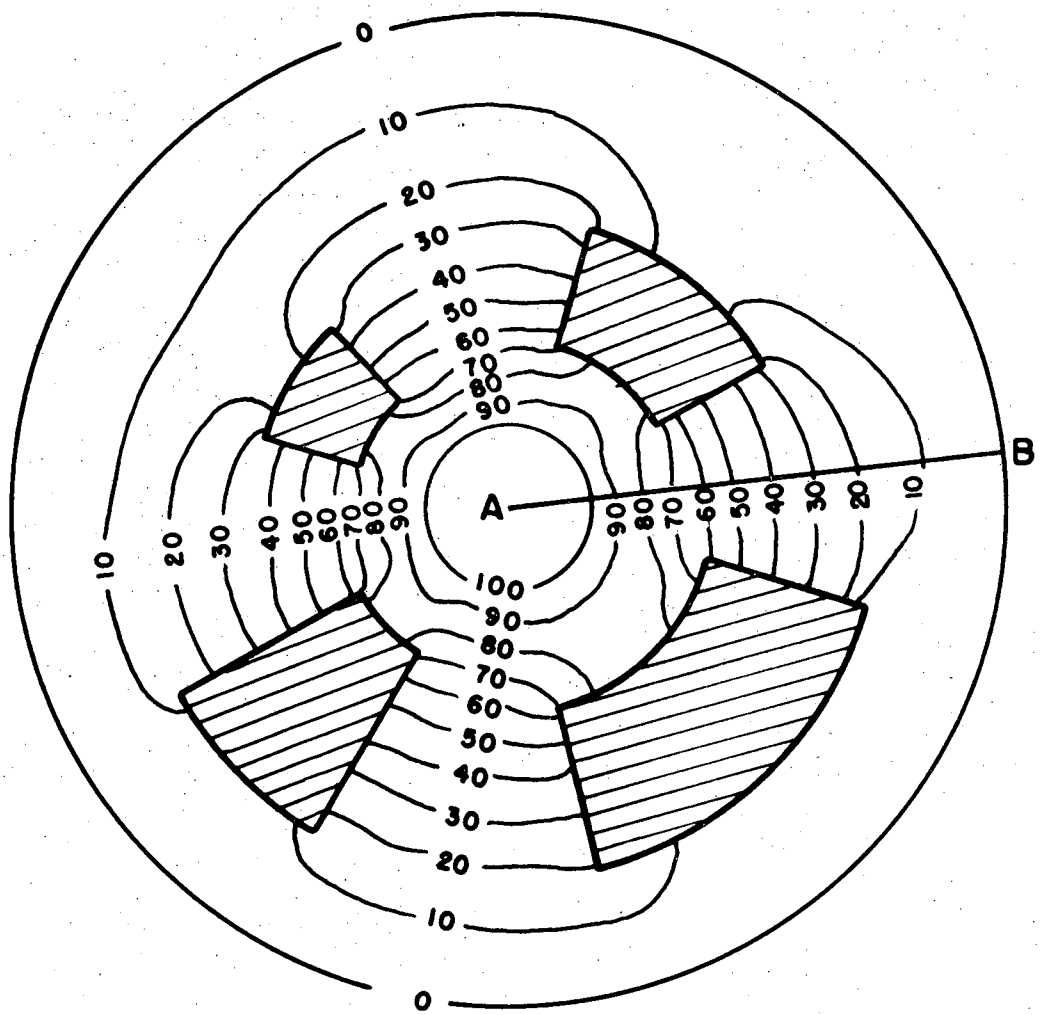

Fig. 7. Pressure distribution in a partially closed fracture

we will analyze the Galerkin formulation of the FEM; and since the IFDM uses a linear approximation for potential gradient, we will restrict our analysis of FEM to "linear" elements.

In the Galerkin scheme, the partial differential equation is first weighted with an appropriate weighting function and then integrated. Thus, after neglecting the source term in (2), we have

$$\int_V \xi_m [\nabla \bullet K \nabla \xi_n \phi_n - c \frac{\partial \xi_n \phi_n}{\partial t}] \, dV = 0 \qquad (14)$$

In writing (14) we have not only expanded divergence and gradient in Cartesian coordinates but also have replaced ϕ by the approximate relation, $\phi \approx \xi_n \phi_n$ where the repetition of n denotes summation over n nodal points. The particular feature of the Galerkin procedure is that the weighting function $\xi_m(x_i)$ is the same as the coordinate function $\xi_n(x_i)$ that is used to approximate ϕ. In the FEM, which is a subdomain scheme, ξ_m is defined as unity at nodal point m and zero at all other nodal points.

In the simplest case involving linear elements, the FEM flow region is discretized into a series of appropriately small triangles, within each of which ϕ is assumed to vary linearly. Thus, ξ_m also varies linearly from a value of 1 at nodal point m to zero along the line connecting the remaining two nodal points of the triangular element. For isotropic media, K in (14) is a scalar; and for anisotropic media, K is a second rank, symmetrical tensor.

Assuming K and c to be constant within each triangular element, and making use of Green's first identity [Sokolnikoff and Redheffer, 1966] we can rewrite (14) as

$$\sum_{\text{all e}} \left\{ - \int_{V^e} \nabla \xi_m \bullet K \nabla \xi_n \phi_n \, dV + \int_{S^e} \xi_m K \nabla \xi_n \phi_n \bullet \vec{n} \, dS - \int_{V^e} \xi_m c \frac{\partial \xi_n \phi_n}{\partial t} \, dV \right\} = 0 \qquad (15)$$

In (15), the superscript e denotes a triangular element and the summation denotes integration over all elements of the flow region. One equation such as (15) is set up for each nodal point m at which the time rate of change of potential is to be determined. Furthermore, the nature of the weighting function ξ_m is such that the surface integral is zero for all interior nodal points. If m lies on a boundary of the flow region where the flux is prescribed, the surface integral becomes a known quantity.

Hence, we need to concern ourselves only with the two volume integrals in Equation 15. Moreover, by definition, ξ_m has nonzero values only in those elements that include nodal point m. Thus, the summation implied in (15) actually means summation only over those triangular elements at whose apex m lies (see Figure 8). For convenience we shall call the subdomain composed of these triangles as the "primary" element of m, while each triangular element will be called a "secondary" element.

Let us now consider the first volume integral in equation 15 as applied to secondary element II in Figure 8. It can be shown [Narasimhan, 1975] that the integral $\int \nabla\xi_m \bullet K\nabla\xi_n\phi_n \, dV$ evaluated with respect to nodal point m is simply the flux normal to the line connecting the mid points A and B of the sides adjacent to m, as shown in Figure 9. Furthermore, if G is the centroid of secondary element II, then, because of the constant gradient of ϕ within the element, the flux across the line AB is exactly equal to the flux across the line AGB. Hence, extending this approach to all secondary elements shown in Figure 8 leads to the conclusion that $\sum_e \int \nabla\xi_m \bullet K\nabla\xi_n\phi_n \, dV$ is a summation of fluxes across the surface enclosing the subregion around nodal point m as shown in Figure 10.

Comparison of Figures 10 and 1 shows that the weighted integration of the spatial integral in the Galerkin scheme and the evaluation of the surface integral in the IFDM both lead to a summation of fluxes across the surface of

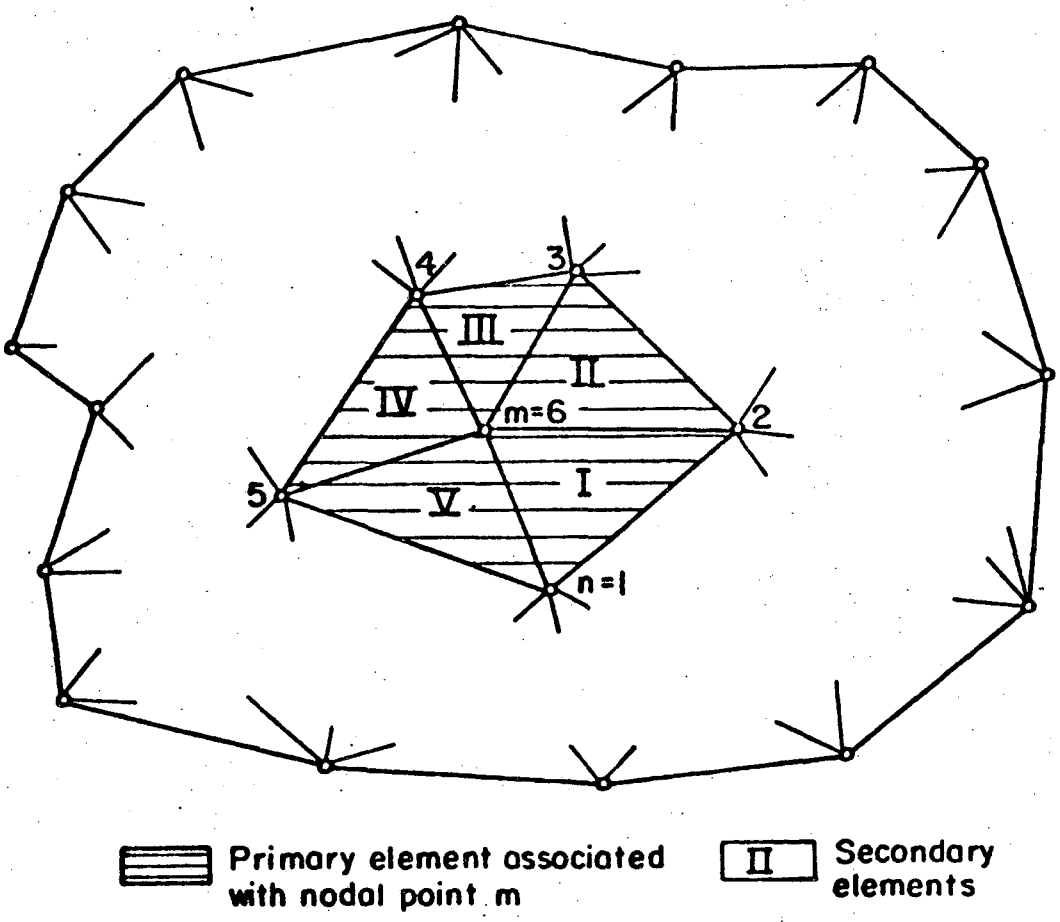

Fig. 8. Primary and secondary elements of a FEM network

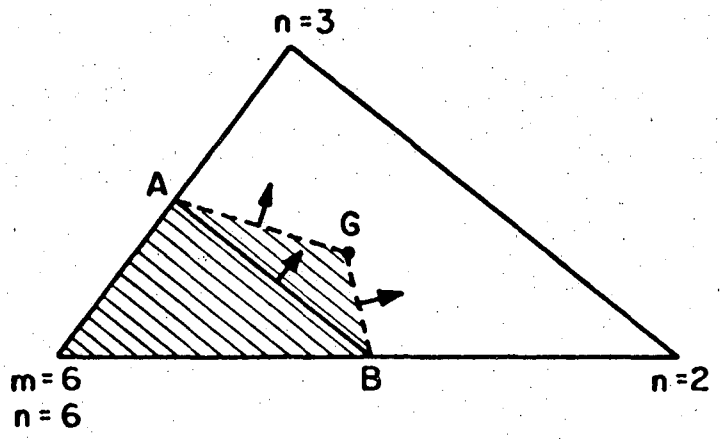

Fig. 9 Expanded view of secondary element II in Figure 8

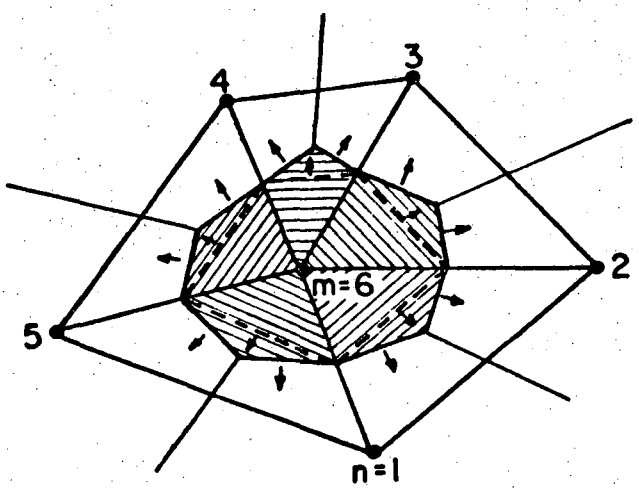

XBL 754-1101

Fig. 10 Evaluation of Galerkin spatial integral for nodal point m

of a subdomain associated exclusively with the nodal point of interest. This summation therefore yeilds the net rate at which fluid is accumulating within the exclusive subdomain associated with nodal point m.

The other volume integral in (15), $\int \xi_m c \frac{\partial \xi_n \phi_n}{\partial t} dV$, determines how the excess fluid accumulating in the exclusive subdomain of nodal point m (Figure 10) is distributed within the subdomain so as to cause ϕ_m to change with time. We will consider two possible ways of interpreting this integral.

First, let us review the conventional Galerkin procedure (equation 14) in which $\xi_n \phi_n$ ($\approx \phi$) is substituted for ϕ in the time derivative. Assuming c is constant within e and recognizing that $\xi_m(x_i)$ is independent of time, we get

$$\sum_e \int_{V^e} \xi_m c \frac{\partial \xi_n \phi_n}{\partial t} dV = \sum_e c^e \int_{V^e} \xi_m \xi_n \frac{\partial \phi_n}{\partial t} dV \qquad (16)$$

Using Felippa's [1966] evaluation of $\int_{V^e} \xi_m \xi_n dV$ for triangular elements, we can rewrite (16) as

$$\sum_e \int_{V^e} \xi_m c \frac{\partial \xi_n \phi_n}{\partial t} dV = \sum_e c^e \left[\frac{\Delta^e}{6} \frac{\partial \phi_m}{\partial t} + \frac{\Delta^e}{12} \left(\frac{\partial \phi_n^1}{\partial t} + \frac{\partial \phi_n^2}{\partial t} \right) \right] \qquad (17)$$

where $\frac{\partial \phi_n^1}{\partial t}$ and $\frac{\partial \phi_n^2}{\partial t}$ are time derivatives at the remaining two nodal points of element e. If we recognize that the shaded subregion associated with nodal point m in Figure 10 is 1/3 the area of the entire pentagon, equation 17 implies that $\frac{\partial \phi_m}{\partial t}$, which is an average value representative of 1/6 of the area of the pentagon, actually denotes the mean rate of change in potential over one half of the shaded subregion in Figure 10. Over the remaining half of this subregion, the fluid is assumed to be distributed in accordance with the average time rates $\frac{\partial \phi_n}{\partial t}$ at the neighboring nodal points of m.

The second way to interpret the integral $\int_{V^e} \xi_m c \frac{\partial \xi_n \phi_n}{\partial t} dV$ is to consider that the net rate of mass accumulation arising out of the first volume integral

in equation 15 is distributed in such a fashion within the shaded subregion in Figure 10 that the time rate of change in potential is uniform throughout. This would imply that in the second volume integral in (15) we should replace $\frac{\partial \xi_n \phi_n}{\partial t}$ by $\frac{\partial \phi^M}{\partial t}$, which is now the mean rate of change in potential over the exclusive subdomain of nodal point m. According to this interpretation, we get instead of (17)

$$\sum_e \int_{V^e} \xi_m c \frac{\partial \phi^M}{\partial t} \, dV = \frac{\partial \phi^M}{\partial t} \sum_e c^e \int_{V^e} \xi_m \, dV = \frac{\partial \phi^M}{\partial t} \sum_e \frac{\Delta^e c^e}{3} \tag{18}$$

The approach suggested by (18) has been used by Neuman [1973] in developing the FEM equations for saturated-unsaturated groundwater flow, involving the solution of non-linear equations. Equation 18 also results from the purely physical development of the FEM equations carried out by Wilson [1968].

When m is an interior nodal point, the surface integral in (15) disappears and, depending on the choice of (17) or (18), the FEM equations can be written in either of the following two forms:

a) The conventional Galerkin form

$$-\sum_e \int_{V^e} \nabla \xi_m \bullet K \nabla \xi_n \phi_n \, dV = \sum_e c^e \left[\frac{\Delta^e}{6} \frac{\partial \phi_m}{\partial t} + \frac{\Delta^e}{12} \left(\frac{\partial \phi_n^1}{\partial t} + \frac{\partial \phi_n^2}{\partial t} \right) \right] \tag{19}$$

or b) The modified Galerkin form:

$$-\sum_e \int_{V^e} \nabla \xi_m \bullet K \nabla \xi_n \phi_n \, dV = \frac{\partial \phi^M}{\partial t} \sum_e \frac{\Delta^e c^e}{3} \tag{20}$$

Comparison of (20) with (5) or (6) shows that conceptually, the modified Galerkin form is almost the same as the IFDM, except for the difference in the

procedure used for evaluating the gradient of ϕ. Comparison of (19) with (5) and (6) shows that the IFDM and the conventional Galerkin procedures are conceptually similar in associating an exclusive subdomain with each nodal point of interest and summing the surface fluxes to evaluate the rate of fluid accumulation within the subdomain. They only differ somewhat in the procedure adopted for redistributing the fluid accumulation over the subdomain.

The interesting fact that emerges out of a comparison of IFDM with FEM is that the chief difference between the two approaches lies in the manner in which the spatial gradients in ϕ are evaluated. As will be seen, the relative advantages and disadvantages of the IFDM and the FEM depend by and large on the technique employed for measuring these gradients.

The IFDM employs the simple finite difference approximation and is thus constrained to measurement of gradients normal to a given surface and is restricted to first order approximations. As a result, it cannot handle general tensorial quantities, since the latter require evaluation of tangential gradients along the reference surface in addition to the normal gradient. Moreover, when the spatial variation of ϕ is rapid, the IFDM would require a large number of mesh points to accurately simulate the rapid variation of ϕ in terms of successive linear segments.

By choosing to set up a surface, $\phi = \xi_n \phi_n$, for the variation of ϕ over an elemental region, the FEM achieves a very general and powerful form of expressing the spatial variation of ϕ. As a result, the FEM is not only well suited for handling general tensorial parameters (e.g., stress, permeability, dispersion) but is also well suited to the utilization of higher order surfaces, which can approximate the rapid spatial variation of ϕ with greater accuracy.

The basic integration scheme in the FEM involves evaluation of volume integrals. Hence, the FEM has to choose, at the outset, a coordinate system

of known symmetry, usually Cartesian. In addition, to facilitate evaluation of the volume integral, the elemental volume has to have a simple shape whose volume can be expressed as a simple function if its dimensions. As a result, when the flow domain has a complex geometry with mixed symmetry, the FEM has to approximate the domain using simple elemental shapes, which may not always be easy. To some extent, this difficulty can be overcome by resorting to higher order, isoparametric elements.

In the case of IFDM which basically evaluates surface fluxes and in which geometrical parameters are provided as input information, there is no restriction on choosing any basic elemental shape. Therefore, arbitrarily shaped elements can be chosen judiciously not only to handle mixed symmetries (as in Figure 3), but also to fit complex boundaries with a small number of elements. A very desirable feature of the IFDM is that it can, in a simple way, handle complex boundaries while still retaining a linear approximation for potential variation.

In the IFDM, care must be taken to design the mesh so that the lines joining nodal points coincide with the normals to the interfaces between the points. This restriction, as well as the requirement for providing geometrical parameters as input data may require added effort in designing networks for complex problems. To some extent this effort can be minimized by developing auxiliary computer programs for mesh and input data generation. On the other hand, the design of the FEM mesh may be less restrictive since the geometric parameters are generated implicitly in the volume integration. However, even in the FEM it may be necessary to have basic elements with some regularity of shape (e.g., avoiding obtuse angled triangles), in order to avoid undesirable matrix properties that affect the efficiency of the solution process.

Certain other differences between IFDM and FEM arise mostly due to the conventions and customary procedures that are followed. If we look at the conventional Galerkin form of the FEM equation (equation 19), we note that the equation for nodal point m also contains the unknown time derivatives at the neighboring nodal points n. Hence, the set of equations arising out of (19) would have to be solved as a set of simultaneous equations involving the unknown time derivatives. In other words (19) cannot be solved explicitly, even for small time steps. On the other hand, the modified Galerkin equation in (20), which is similar to the IFDM equations (5) or (6), can be solved explicitly or implicitly.

In addition to their simplicity, an added advantage of IFDM equations is that stability conditions are easier to define (equation 8) and this has enabled the development of an optimal explicit-implicit procedure used in the program TRUMP. The IFDM has also been amenable to the development of a successful iterative scheme, that has produced satisfactory results for a wide class of problems [Edwards, 1969; Narasimhan, 1975]. The result of using such a scheme is that IFDM is not constrained by the need for optimal numbering of nodal points. Furthermore, a single computer program is able to handle one-, two- or three-dimensional problems and the size of a problem does not necessarily depend on its dimensionality.

Although iterative schemes are occasionally used in the FEM, solutions are normally obtained with matrix-inversion techniques. Matrix inversion schemes are more accurate than iterative schemes, especially in the case of matrices which are not very well behaved. However, such inversion techniques are generally constrained by the need for an optimal nodal point numbering and by the need for keeping band width small in order to conserve computer storage. The latter may often prove to be a handicap in handling reasonably large

three-dimensional problems with the FEM.

From the above discussion of IFDM and FEM, we have seen that some of the differences are intrinsic in the methods used while others are mainly a matter of convention. If suitable changes in convention could be made, it would appear that one could combine the advantages of both methods and develop an improved numerical process.

As was discussed earlier, the modified Galerkin approach (equation 20) is conceptually very similar to equations 5 or 6 in the IFDM. It would appear, therefore, that the stability criterion for IFDM given by (8) should be equally applicable to (20). For the same reason, it also seems likely that the iterative procedure used in TRUMP could be successfully applied to the modified Galerkin equation. This suggests that, a priori, there is good reason to attempt to develop an FEM code with linear elements using an explicit-implicit, iterative solution scheme. The advantages of such an approach are obvious. In addition to using the simple explicit procedure wherever possible, one could handle multi-dimensional problems as well as problems with complex geometry without being constrained by either an optimal scheme for nodal point numbering or by the size of band width.

Conclusions

The theoretical basis for the integrated finite difference method reveals a rather simple but powerful numerical technique for solving groundwater flow problems. Examples have been provided to demonstrate that the IFDM as incorporated in TRUMP can handle two- or three-dimensional problems with ease.

A comparison of IFDM and FEM indicates that each of these integral methods has distinct advantages in handling certain classes of problems. The modified Galerkin form of the FEM is conceptually almost the same as the IFDM, except

for the difference in the procedure used in evaluating the gradient of ϕ. This suggests the possibility of developing a new FEM code that can incorporate the explicit-implicit iterative solution scheme in TRUMP and thus combine the advantages that are inherent in both IFDM and FEM.

Acknowledgements

We would like to thank Dr. T. J. Lasseter and Dr. S. P. Neuman for many fruitful discussions during the preparation of this paper. We also appreciate the assistance of Mr. Katsuhiko Iwai in providing the solution for the fracture flow problem. This work was partially supported by the U. S. Atomic Energy Commission.

References

Carslaw, H. S. and J. C. Jaeger, Conduction of Heat in Solids, Oxford, Clarendon Press, p. 261, 1959.

Cooley, R. L., "A finite difference method for variably saturated porous media: Application to a single pumping well", Water Resources Res., 7(6), 1607-1625, 1971.

Dusinberre, G. M., Heat Transfer Calculations by Finite Differences, International Text Book Co., Scranton, Pennsylvania, 1961.

Edwards, A. L., TRUMP: A Computer Program for Transient and Steady State Temperature Distributions in Multidimensional Systems, National Tech. Inf. Ser., National Bureau of Standards, Springfield, Virginia 22151, 1969.

Encyclopedia of Science and Technology, 5, p. 45, McGraw Hill, 1960.

Evans, G. W., R. J. Brousseau and R. Keirstead, Instability Considerations for Various Difference Equations Derived from the Diffusion Equation, Rept. UCRL-4476, Lawrence Radiation Laboratory, Livermore, 1954.

Felippa, C. A., Refined Finite Element Analysis of Linear and Nonlinear Two-dimensional Structures, Rept. No. SESM 66-22, Department of Civil Engineering, University of California, Berkeley, 1966.

Gale, J. E., R. L. Taylor, P. A. Witherspoon and M. S. Ayatollahi, "Flow in rocks with deformable fractures", in Finite Element Methods in Flow Problems, editors J. T. Oden et al., UAH Press, Alabama, 583-598, 1974.

Javandel, I. and P. A. Witherspoon, "Application of the finite element method to transient flow in porous media", Soc. Petrol. Eng. Journ. 8 (3), 241-250, 1968.

Louis, C., A Study of Groundwater Flow in Jointed Rock and its Influence on the Stability of Rock Masses, Rock Mechanics Research Report No. 10, Imperial College, University of London, 1969.

MacNeal, R. H., "An asymmetric finite difference network", Quart. Appl. Math., II, 295-310, 1953.

Narasimhan, T. N., A Unified Numerical Model for Saturated-Unsaturated Groundwater Flow, Ph.D. dissertation, Department of Civil Engineering, University of California, Berkeley, 1975.

Neuman, S. P., "Saturated-unsaturated seepage by finite elements", Journ. Hydr. Div., ASCE, 99 (HY12), 2233-2250, 1973.

O'Brien, G. G., M. A. Hyman and S. Kaplan, "A study of the numerical solution of partial differential equations", Journ. Math. Phys. 29, 223-251, 1951.

Pinder, G. F. and E. O. Frind, "Application of Galerkin procedure to aquifer analysis", Water Resources Res., 8 (1), 108-120, 1972.

Romm, E. S., Flow Phenomena in Fractured Rocks (in Russian), Nedra, Moscow, 1966.

Sharp, J. C. and Y. N. T. Maini, "Fundamental considerations on the hydraulic characteristics of joints in rock", in Proceedings of Symposium on Percolation through Fissured Rock, Stuttgart, T1-F, 1-15, 1972.

Snow, D. T., A Parallel Plate Model of Fractured Permeable Media, Ph.D. dissertation, Department of Civil Engineering, University of California, Berkeley, 1965.

Sokolnikoff, I. S. and R. M. Redheffer, Mathematics of Physics and Modern Engineering, McGraw Hill, New York, 1966.

Theis, C. V., "The relation between the lowering of the piezometric surface and the rate of duration and discharge of a well using groundwater storage", Trans. Am. Geophys. Union, 16, 519-524, 1935.

Todd, D. K., Ground Water Hydrology, John Wiley, New York, 1959.

Wilson, C. R. and P. A. Witherspoon, "Steady state flow in rigid networks of fractures", Water Resources Res., 10 (2), 328-335, 1974.

Wilson, E. L., The Determination of Temperatures within Mass Concrete Structures, SESM Report No. 68-17, Department of Civil Engineering, University of California, Berkeley, 1968.

Zienkiewicz, O. C. and C. J. Parekh, "Transient field problems: Two-dimensional and three-dimensional analysis by isoparametric finite elements", Int. Journ. Num. Meth. in Eng., 2, 71-71, 1970.

Nomenclature

$A_{m,n}$	Area of interface between elements m and n in IFDM $[L]^2$
b	Fracture aperture [L]
c	Specific fluid capacity or specific storage [1/L]
$D_{m,n}$	Distance between nodal points m and n in IFDM
g	i) Flow rate per unit volume [1/T] ii) Acceleration due to gravity in fracture flow problem $[L/T^2]$
g_m	Flow rate per unit volume of element m [1/T]
K	Hydraulic conductivity [L/T]
$\bar{K}_{m,n}$	Mean hydraulic conductivity between elements m and n [L/T]
m	Subscript used to denote an element or a nodal point [1]
n	Subscript used to denote an element or a nodal point [1]
$\vec{n}$	Unit outer normal to a surface [1]
Q	Flow rate $[L^3/T]$
r	Radial distance [L]
r^e	Radial distance to external boundary in fracture flow problem [L]
r_i	Radial distance to internal boundary in fracture flow problem [L]
S	i) Storage coefficient in Theis equation [1] ii) Surface of integration
t	Time [T]
T	Coefficient of transmissibility in Theis equation $[L^2/T]$
$U_{m,n}$	Conductance between elements m and n $[L^2/T]$
V	Volume $[L^3]$
V_m	Volume of element m $[L^3]$
Δ^e	Area of triangular element e
κ	Diffusivity $[L^2/T]$
λ	Weight given to the backward differencing operation in the implicit scheme [1]

μ Viscosity of fluid [M/LT]

ξ Function to express the variation of potential over an element e in the FEM; Also the Galerkin weighting function [1]

ξ_m Weighting function pertaining to nodal point m

ρ Density of fluid [M/L^3]

ϕ Fluid potential or hydraulic head [L]

TECHNICAL INFORMATION DIVISION
LAWRENCE BERKELEY LABORATORY
UNIVERSITY OF CALIFORNIA
BERKELEY, CALIFORNIA 94720